

EEG-36  
DOE/AL/10752-36

POST BURIAL ALTERATION OF THE PERMIAN  
RUSTLER FORMATION EVAPORITES,  
WIPP SITE, NEW MEXICO: TEXTURAL  
STRATIGRAPHIC AND CHEMICAL EVIDENCE

Tim K. Lowenstein  
Consultant

Environmental Evaluation Group  
Environmental Improvement Division  
Health and Environment Department  
P. O. Box 968  
Santa Fe, New Mexico 87503

April 1987

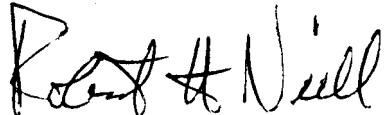
## FOREWORD

The purpose of the Environmental Evaluation Group (EEG) is to conduct an independent technical evaluation of the potential radiation exposure to people from the proposed Federal Radioactive Waste Isolation Pilot Plant (WIPP) near Carlsbad, in order to protect the public health and safety and ensure that there is minimal environmental degradation. The EEG is part of the Environmental Improvement Division, a component of the New Mexico Health and Environment Department -- the agency charged with the primary responsibility for protecting the health of the citizens of New Mexico.

The Group is neither a proponent nor an opponent of WIPP.

Analyses are conducted of available data concerning the proposed site, the design of the repository, its planned operation, and its long-term stability. These analyses include assessments of reports issued by the U. S. Department of Energy (DOE) and its contractors, other Federal agencies and organizations, as they relate to the potential health, safety and environmental impacts from WIPP.

The project is funded entirely by the U. S. Department of Energy through Contract DE-AC04-79AL10752 with the New Mexico Health and Environment Department.

  
Robert H. Neill  
Director

EEG STAFF

James K. Channell<sup>(1)</sup>, Ph.D., P.E., Environmental Engineer  
Jenny B. Chapman, M.S., Hydrogeologist  
Lokesh Chaturvedi, Ph.D., Engineering Geologist  
Jim Kenney, M.S., Environmental Scientist  
C. Robert McFarland, B.S., Quality Assurance Engineer  
Robert H. Neill, M.S., Director  
Michael J. Norfleet, Environmental Technician  
Teresa Ortiz, Administrative Secretary  
John C. Rodgers, Ph.D., Health Physicist  
Carol Shope, B.A., Secretary III  
Norma Silva, Administrative Officer  
Dyana Todd, M.L.S., Librarian

---

(1) Certified, American Board of Health Physics

CONTENTS

<u>Title</u>	<u>Page</u>
Foreword.....	i
EEG Staff.....	ii
Contents.....	iii
List of Figures and Photographs.....	iv
Preface .....	vii
Acknowledgements.....	x
INTRODUCTION.....	1
GEOLOGIC SETTING.....	6
SYNDEPOSITIONAL FEATURES, INTERPRETATION OF DEPOSITIONAL ENVIRONMENTS AND DIAGENETIC OVERPRINTS.....	7
Lower Member.....	7
Culebra Dolomite Member.....	19
Tamarisk Member.....	21
Forty Niner Member.....	26
CRITERIA FOR RECOGNIZING LATE STAGE ALTERATION.....	29
Evidence for late-stage chemical alteration.....	31
Evidence for late-stage physical alteration.....	31
DISSOLUTION OF EVAPORITES IN THE RUSTLER FORMATION.....	34
Possibility of present day dissolution.....	36
REFERENCES.....	40

## FIGURES AND PHOTOGRAPHS

### Figures

	<u>Title</u>	<u>Page</u>
1.	Outline of the approximate aerial extent of the Rustler Formation, from Hills (1942, p. 243) and Hills (1972, p. 2319).....	2
2.	Location of WIPP site, the four borehole cores examined and Well P-18.....	3
3.	Distances between the four borehole cores examined and Well P-18.....	4
4(a).	Stratigraphic Columns - Lower Member Rustler Formation.....	8
4(b).	Legend for Figure 4(a).....	9
5(a).	Stratigraphic columns, Culebra Dolomite Member and Tamarisk Member, Rustler Formation.....	10
5(b).	Legend for Figure 5(a).....	11
6(a).	Stratigraphic columns - Magenta and Forty-Niner Members, Rustler Formation.....	12
6(b).	Legend for Figure 6(b).....	13

### Photographs

	<u>Title</u>	<u>Page</u>
1.	Very-fine grained, muddy sandstone, with lamination disrupted by burrows. S-1 siliciclastic sandstone and mudstone, Lower Member.....	44
2.	Very fine grained laminated muddy sandstone near top of S-1 siliciclastic sandstone and mudstone sequence, Lower Member.....	44
3.	Laminated to thin bedded mudstone and very fine grained sandstone, with isolated randomly oriented subhedral to euhedral halite cubes. Near base of the muddy halite (H-1) of the Lower Member.....	44

Photographs (continued)

	<u>Title</u>	<u>Page</u>
4.	Mudstone-halite from muddy halite (H-1) of the Lower Member.....	44
5.	Layered halite from the anhydrite-halite sequence (A-H-1) of the Lower Member.....	46
6.	Mudstone-halite from muddy halite (H-2) of the Lower Member.....	46
7.	Laminated anhydrite from anhydrite (A-1) of the Lower Member.....	46
8.	Contact between anhydrite (A-1) and mudstone (I) of the Lower Member.....	46
9.	Mudstone (I) of the Lower Member.....	48
10.	Dolostone from near base of Culebra Dolomite Member...	48
11.	Structureless dolostone from middle part of Culebra Dolomite Member.....	48
12.	Halite from halite-muddy halite sequence (H-3) of the Tamarisk Member.....	48
13.	Brown mudstone (II) of the Tamarisk Member.....	50
14.	Chaotic mudstone from Mudstone II of the Tamarisk Member.....	50
15.	Brown mudstone II of the Tamarisk Member.....	50
16.	Base of anhydrite (A-3) of the Tamarisk Member.....	50
17.	Middle portion of anhydrite (A-3) of the Tamarisk Member.....	52
18.	Laminated dolostone from base of the Magenta Dolomite Member.....	52
19.	Laminated dolostone from base of Magenta Dolomite Member.....	52
20.	Laminated to thin bedded dolostone with dark, organic-rich(?) partings from the Magenta Dolomite Member.....	52

Photographs (continued)

	<u>Title</u>	<u>Page</u>
21.	Large scale cross stratification in the Magenta Dolomite Member.....	54
22.	Bottom of anhydrite (A-5), Forty-Niner Member.....	54
23.	Uppermost portion of A-5 anhydrite, Forty-Niner Member.....	54
24.	Contact between gypsum of the A-5 anhydrite of the Forty-Niner Member (top of Rustler Formation) and the structureless brown mudstone of the Dewey Lake Formation.....	54

## PREFACE

A repository for permanent isolation of defense transuranic wastes is being excavated in southeastern New Mexico, about 40 km (25 miles) east of Carlsbad. The Waste Isolation Pilot Plant (WIPP) repository has been designed for the disposal of waste in the lower part of the Salado (salt) Formation at a depth of 655 meters (2150 ft). The water-bearing zones of the Rustler Formation, which overlies the Salado, are considered to be the main pathway for the transport of radionuclides to the biosphere, if the repository is breached.

The Rustler Formation is 150 meters (490 ft) thick, 6.4 Km (4 miles) east of the center of the WIPP site. The thickness reduces drastically to the west so that it is only 91 meters (300 ft) thick in the western part of the WIPP site. At its thickest location, the Rustler consists of siltstone and anhydrite with two dolomite beds and both clear and clayey halite. Halite is progressively missing from deeper layers from east to west in the Rustler cross-section across the WIPP site. These observations were interpreted by Powers et al (1978), Mercer (1983), Lambert (1983), Chaturvedi and Rehfeldt (1984), Bachman (1984), Snyder (1985), Chaturvedi and Channell (1985) and others as indicating post-burial dissolution of halite and increased gypsification of anhydrite further west. Increased permeability of the water-bearing dolomites from east to west also was thought to result from the increased fracturing as a result of dissolution.

In 1984, Powers and Holt (1984) and Holt and Powers (1984) expressed doubts about the concept of post-burial dissolution of Rustler evaporites, on the basis of detailed mapping in the WIPP Waste Handling Shaft, and stated the following:



"Post-depositional dissolution features were not observed in any stratigraphic horizons in the Waste Shaft. In fact, several zones previously identified as dissolution residues in nearby boreholes (e.g. ERDA-9) contain pronounced primary sedimentary features. This is of great significance since dissolution has, historically, been considered as an important process that has greatly modified the Rustler Formation in this area." (Holt and Powers, 1984).

This statement was based on the first detailed sedimentological study of the Rustler stratigraphy, but only at one location, albeit in situ, in a shaft. It clearly signaled the need for further work on the lateral variations in the stratigraphy of the Rustler Formation across the WIPP site. Since the interpretation by Powers and Holt was based on sedimentary features, the need was for a sedimentological study of the Rustler Formation.

To resolve this issue, the Environmental Evaluation Group (EEG) asked Dr. Tim K. Lowenstein to perform a sedimentological study of the available cores of the Rustler Formation. Dr. Lowenstein is a sedimentologist with special interest in the study of evaporites and has studied the Ochoan evaporites of the Delaware Basin (Lowenstein, 1982, 1985). For this study, he performed a detailed sedimentological analysis of the Rustler cores from four wells, viz. DOE-2, W-19, H-11 and H-12. This included visual examination of the cores, preparation and petrographic analyses of 52 thin sections from selected locations of the cores, and x-ray diffraction analyses of 40 samples from selected locations of the cores. In addition, descriptive data on the rock cuttings and geophysical logs of borehole P-18 were used for correlation purposes. This report is a result of these

analyses and correlation of sedimentary features between the drill-holes.

This study was confined to a miniscule area (only about 0.05%) of the total extent of the Rustler Formation and therefore cannot be considered to be a study of post-burial alteration of the Rustler Formation as a whole. Within the confines of this area, however, detailed stratigraphic correlations by Dr. Lowenstein based on sedimentary structures and textures indicate overall uniformity of depositional setting. Further, the physical and chemical alteration features, based on crosscutting relations, represent the last processes which have operated on these rocks. Four distinct dissolution zones in the Rustler Formation have been interpreted by Dr. Lowenstein. Although the strata above and below the inferred dissolution zones are chemically and physically altered, they contain abundant sedimentary structures and an internal stratigraphy that can easily be matched from well to well. Dr. Lowenstein does not see a contradiction between post depositional dissolution and the survival of sedimentary structures. His interpretation is that the dissolved species produced by solution are removed from the site of reaction and the zones in which the effects of dissolution are now seen were at the periphery of main dissolution activity and therefore may exhibit some alteration as well as primary sedimentary structures.

- Lokesh Chaturvedi

#### ACKNOWLEDGMENTS

The author wishes to express his sincere appreciation to Dr. Dennis W. Powers and Mr. Robert M. Holt of the University of Texas at El Paso for their help in preparing the cores for study and for fruitful exchanges of opinions on the interpretation of sedimentary features as seen in the cores. Dr. Lokesh Chaturvedi and Ms. Jenny B. Chapman of the Environmental Evaluation Group reviewed the report and made many helpful suggestions for improvement. Ms. Georgia Bayliss drafted the figures with meticulous care and Ms. Teresa Ortiz painstakingly and cheerfully typed several drafts of the report. Dr. Chaturvedi saw the report through the publication stages.

## INTRODUCTION

The Rustler Formation is a Late Permian (Ochoan Series) evaporite found in the subsurface and in outcrop in New Mexico and West Texas (Fig. 1). It occurs over an area in excess of 100,000 km<sup>2</sup> with known thicknesses of up to 150m. The main rock types of the Rustler Formation are anhydrite, gypsum, halite, dolostone and siliciclastic sandstone and mudstone. Across the WIPP site, located in southeastern New Mexico (Fig. 1), some of the Rustler rock types and their thicknesses change dramatically over short lateral distances. These lateral variations have mainly been attributed to post-burial dissolution of evaporites (Powers et al., 1978; Chaturvedi and Rehfeldt, 1984; Snyder, 1985). Recently, Powers and Holt (1984) have challenged this interpretation, based on the excellent preservation of primary sedimentary features in much of the Rustler Formation. From their studies, Powers and Holt (1984) raise the possibility that the lateral changes in thickness and rock types of the Rustler Formation may reflect original sedimentary facies variations.

The aim of the present study is to distinguish syndepositional features from post burial alteration features in the Rustler Formation. Such an investigation then allows testing of the "primary sedimentary" versus "post-burial dissolution" hypotheses just discussed. Four borehole cores of the complete Rustler Formation were examined in hand samples and in thin sections (Figs. 2 and 3). Mineral identification was confirmed by x-ray diffraction analysis. For each cored section of the Rustler Formation, primary sedimentary structures, textures and fabrics were identified, based on comparison with modern evaporite deposits. Vertical and lateral patterns of primary sedimentary features were recorded. From this information, depositional

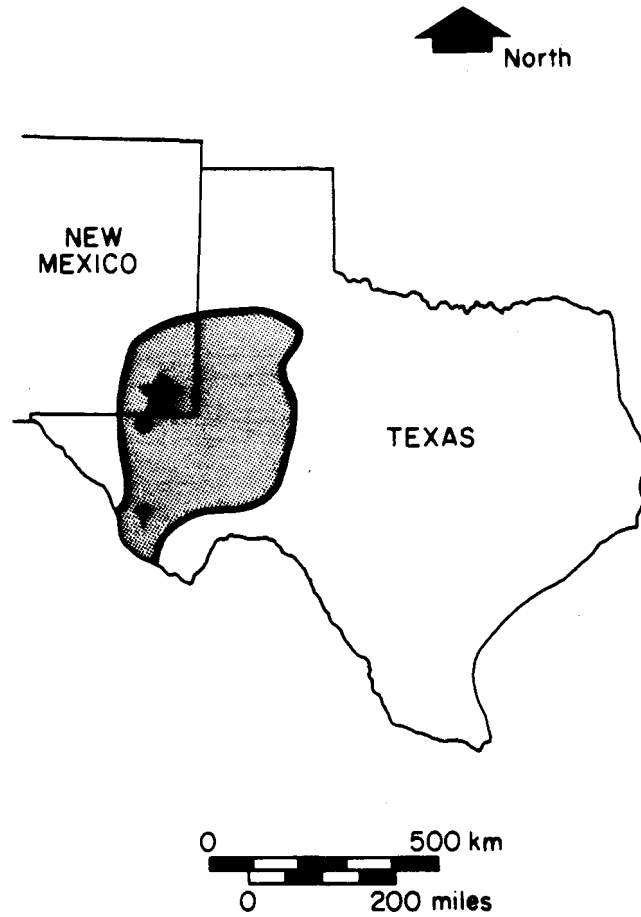


Figure 1. Outline of the approximate aerial extent of the Rustler Formation, from Hills (1942, p. 243) and Hills (1972, p. 2319). The area to the southwest is largely inferred (?), but has been interpreted as the dominant late Permian (Ochoan) marine connection. Dark circle is study area of Walter (1953) and the star represents the location of the WIPP site.

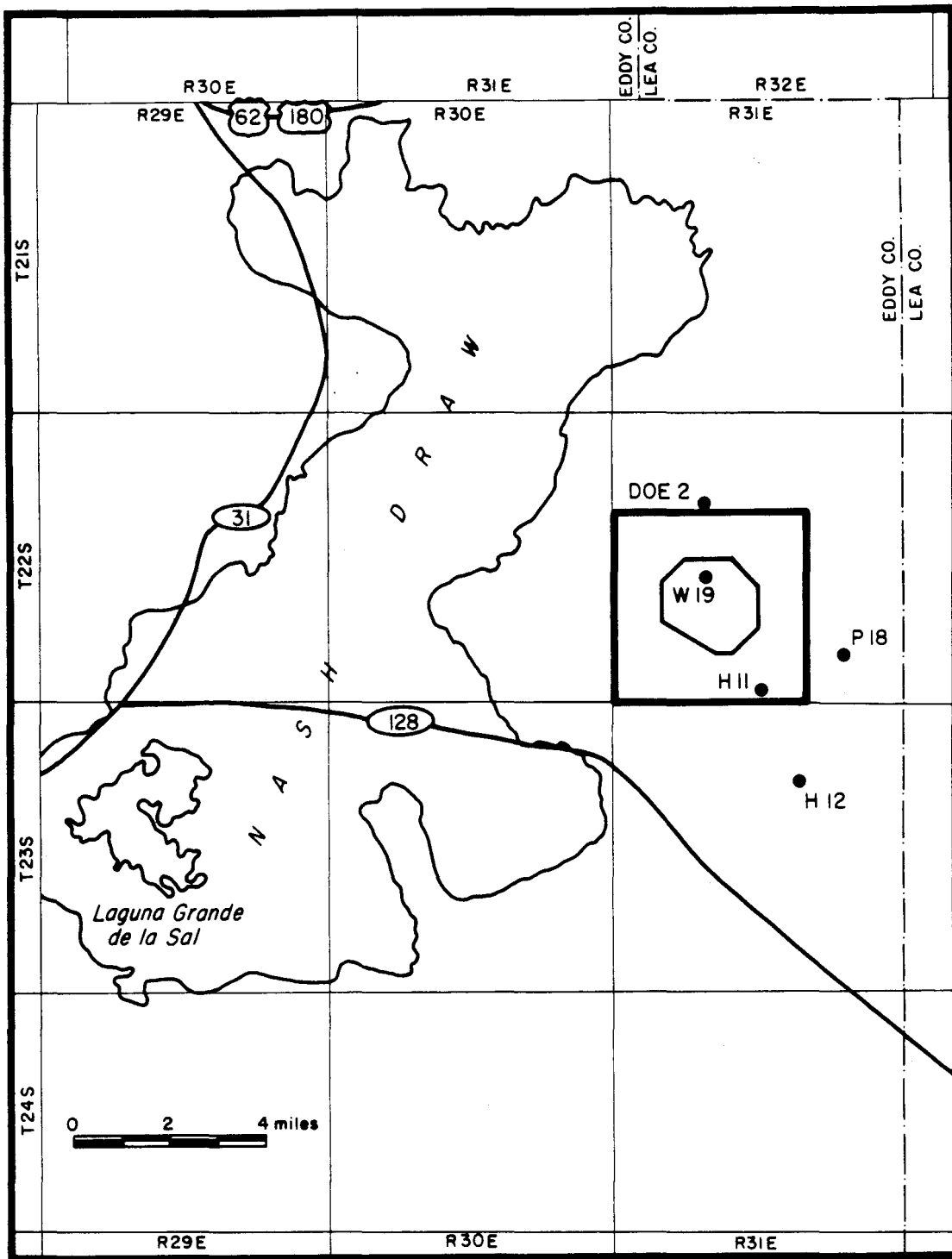


Figure 2. Location of WIPP site, the four borehole cores examined and Well P-18.

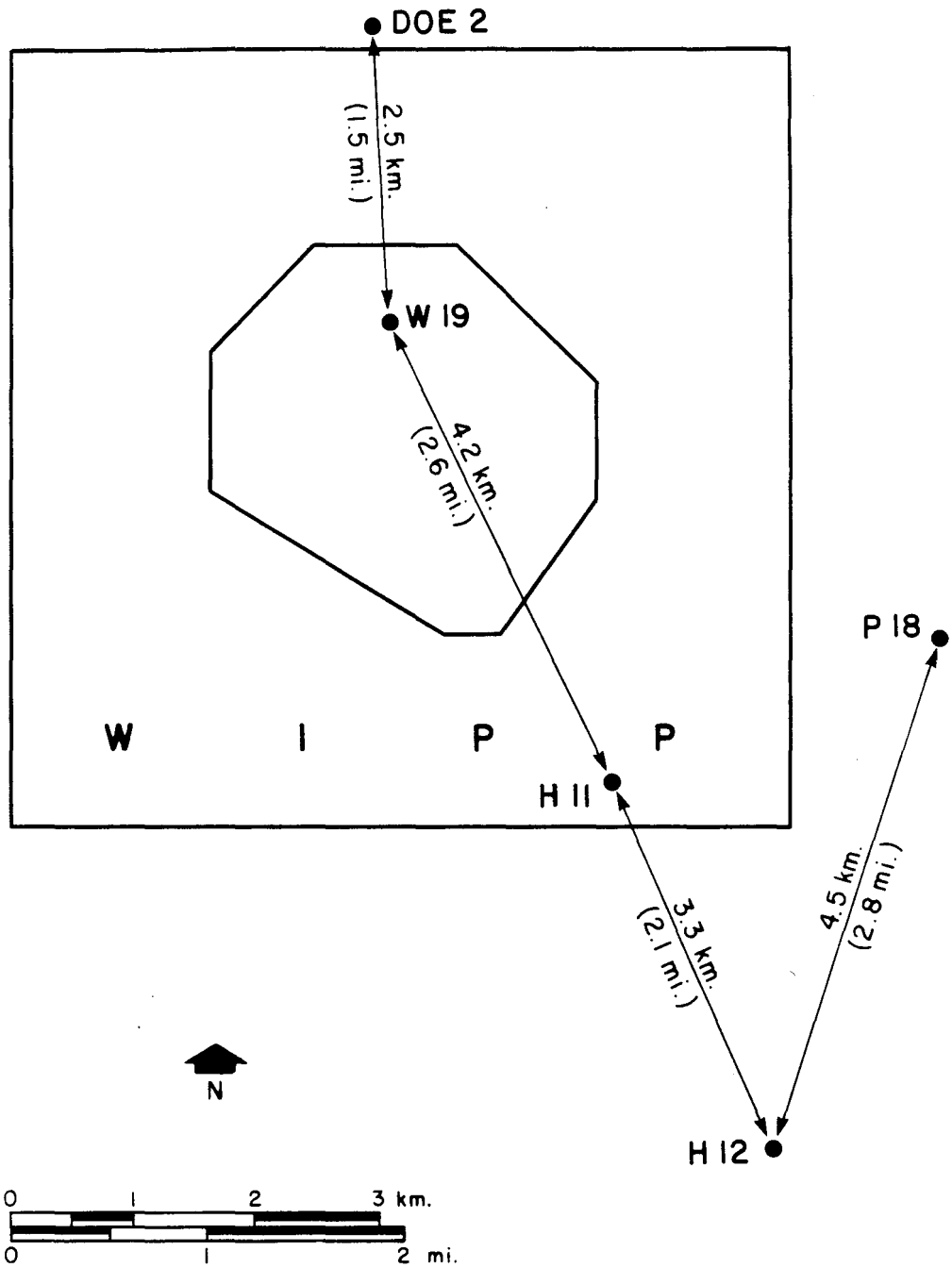


Figure 3. Distances between the four borehole cores examined and Well P-18.

settings have been assembled which best account for the observed types of primary features and their vertical and lateral distribution. With this framework, post-depositional diagenetic overprints were identified in the Rustler Formation. These diagenetic features include mineral replacements (dolomitization, conversion of gypsum to anhydrite or anhydrite to gypsum), mineral precipitation (cements, fracture-fillings), and deformation features such as fracturing and faulting. Dissolution of gypsum, anhydrite and halite is interpreted to have occurred in some portions of the Rustler Formation. The relative timing of these alteration features can commonly be deduced from textural studies, but the absolute timing of alteration cannot be obtained by this method. However, based on comparison of the observed alteration features with the present-day chemical composition of the Rustler Formation waters, the question of whether subsurface diagenetic alteration is presently active at the WIPP site is addressed.



## GEOLOGIC SETTING

The Rustler Formation is part of the Late Permian Ochoan Series of West Texas and eastern New Mexico which includes, from bottom to top, the Castile Formation, the Salado Formation, the Rustler Formation and the Dewey Lake Formation. These rocks, totalling over 1300m in thickness are, with the exception of the siliciclastic redbeds of the Dewey Lake Formation, dominated by evaporites. In the area of the WIPP site in southeastern New Mexico, the Rustler Formation is up to 150m thick and its stratigraphy is well known. Outside this small area, little detailed study of the Rustler Formation has been done. On the eastern edge of the basin, Page and Adams (1940) state that Rustler anhydrites grade laterally into redbeds. Outcrop studies southwest of the WIPP site by Walter (1953) show that in Culberson County, Texas, the lower part of the Rustler Formation is predominantly dolostone, limestone and siltstone (Fig. 1). Significantly, marine invertebrate fossils were discovered by Walter (1953) which firmly establishes the Rustler Formation as at least partly marine in origin. The western edge of the Rustler Formation is an eroded/dissolution boundary so its original western limit is uncertain.

SYNDEPOSITIONAL FEATURES, INTERPRETATION OF DEPOSITIONAL  
ENVIRONMENTS AND DIAGENETIC OVERPRINTS

The stratigraphic sequence of the Rustler Formation in the four borehole cores is shown in Figures 4, 5 and 6. In general, the sequence is similar across the WIPP site. One additional well, P-18, is included in the figures, but rock types were identified from well cuttings and geophysical logs by Jones (1978) and Snyder (1985). The rock types of the Rustler Formation are described below from bottom to top.

The contact between the underlying Salado Formation and the Rustler Formation was examined in three cores, DOE-2, WIPP-19 and H-12. The top of the Salado Formation contains meter-scale sequences of halite and muddy halite similar to those described by Lowenstein (1982). Above the top halite of the Salado Formation is a thin transition zone, 0.7 to 0.9m in thickness, which is composed of interlayered anhydrite and mudstone followed above by vaguely laminated brown mudstone.

LOWER MEMBER

The lower member of the Rustler Formation contains in ascending order: siliciclastic mudstone and very fine grained sandstone (S-1), muddy halite (H-1), interbedded anhydrite and halite (A-H-1), muddy halite (H-2), anhydrite (A-1) and mudstone (I) (Fig. 4). The same detailed stratigraphic sequence occurs in all four cores and in the published descriptions of well P-18 to the east of the WIPP site. One notable exception is the mudstone (I), which in well P-18 probably consists of muddy halite (Fig. 4). Most of the Lower Member is probably equivalent to the outcrop sections of dolostone, siltstone and limestone in Culberson County, Texas (Walter, 1953).

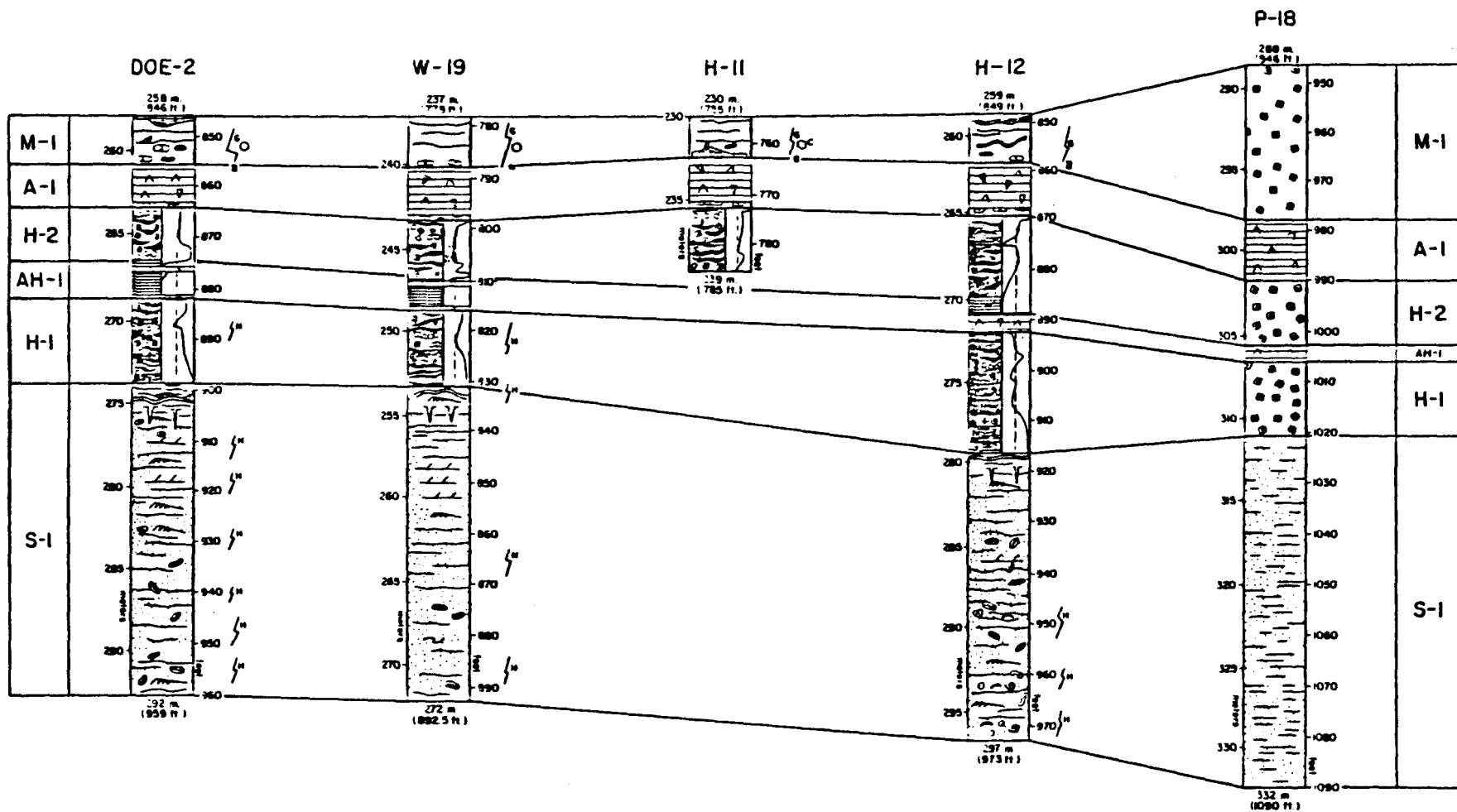
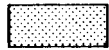


Figure 4(a). Stratigraphic Columns - Lower Member Rustler Formation  
(See Fig. 4b for legend)

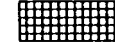
## ROCK TYPES



Mudstone



Anhydrite



Halite



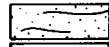
Very fine grained sandstone and mudstone



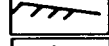
Muddy halite

## SEDIMENTARY AND DIAGENETIC FEATURES

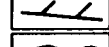
S-1



Mottled very fine grained sandstone/mudstone



Cross lamination



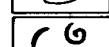
Cross bedding



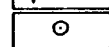
Contorted layering



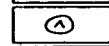
Prism cracks



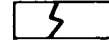
Burrows



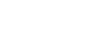
Shells



Coated grains/oolites

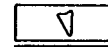


Anhydrite nodules



Halite-filled fractures

A·H·1, A·1

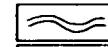


Gypsum pseudomorphs



Gypsum

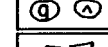
M·1



Contorted layering



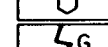
Mudstone fragments



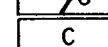
Gypsum/anhydrite fragments



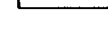
Brecciation



Gypsum crystals



Gypsum filled fractures



Disseminated calcite

H·1, H·2



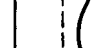
Displacive halite crystals



Halite crystal aggregates



Discontinuous mudstone layers



Approximate percentage mudstone  
in muddy halite

0 50 100%

Figure 4(b). Stratigraphic columns - Lower Member Rustler Formation.  
(Legend for Fig. 4a)

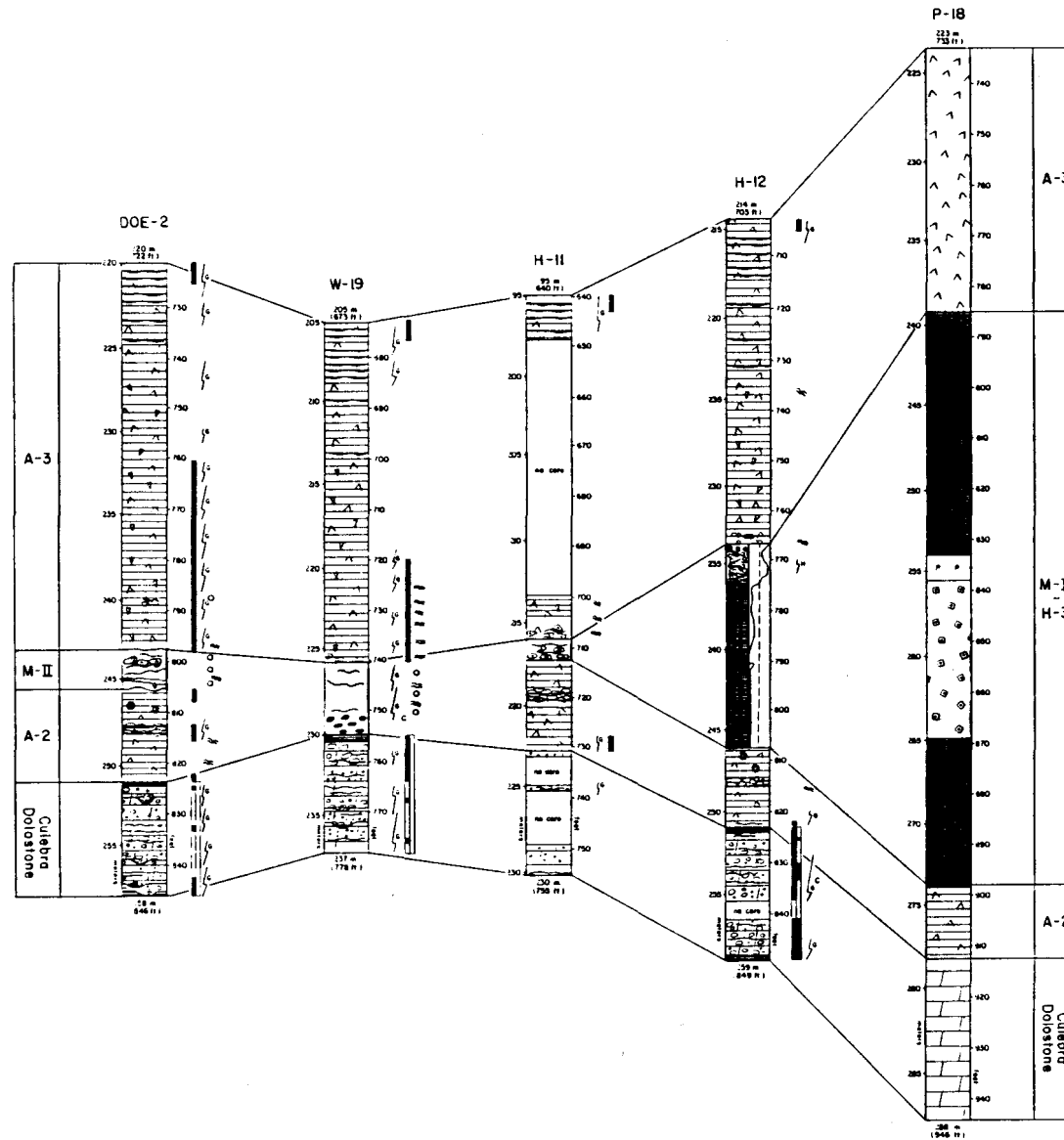
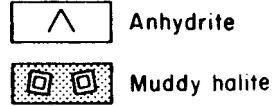
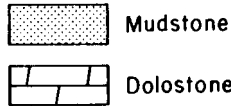


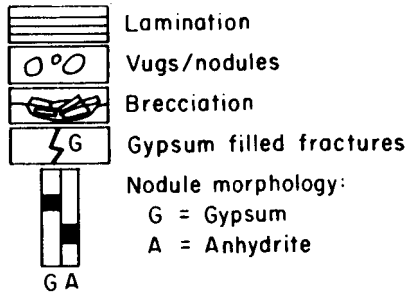
Figure 5(a). Stratigraphic columns, Culebra Dolomite Member and Tamarisk Member, Rustler Formation (See Fig. 5b for Legend)

**ROCK TYPES**

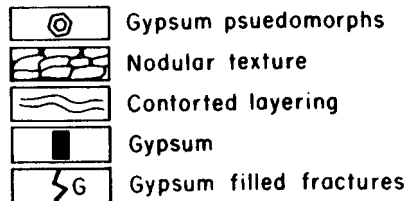


**SEDIMENTARY AND DIAGENETIC FEATURES**

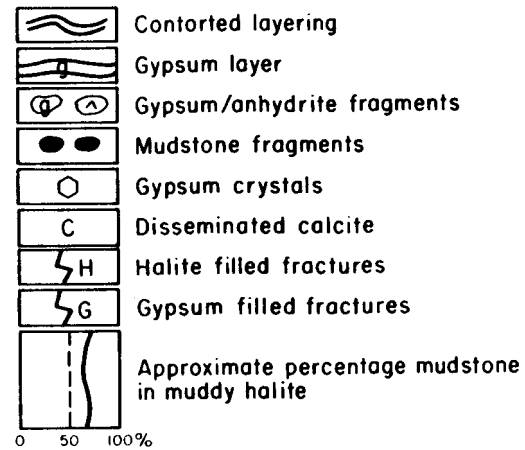
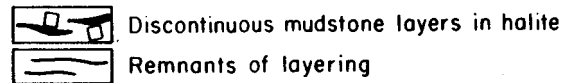
**CULEBRA DOLOSTONE**



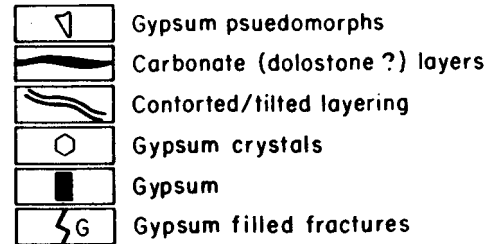
**A-2**



**M-II-H-3**



**A-3**



-11-

Figure 5(b). Stratigraphic columns, Culebra Dolomite Member and Tamarisk Member, Rustler Formation. (Legend for Fig. 5a)

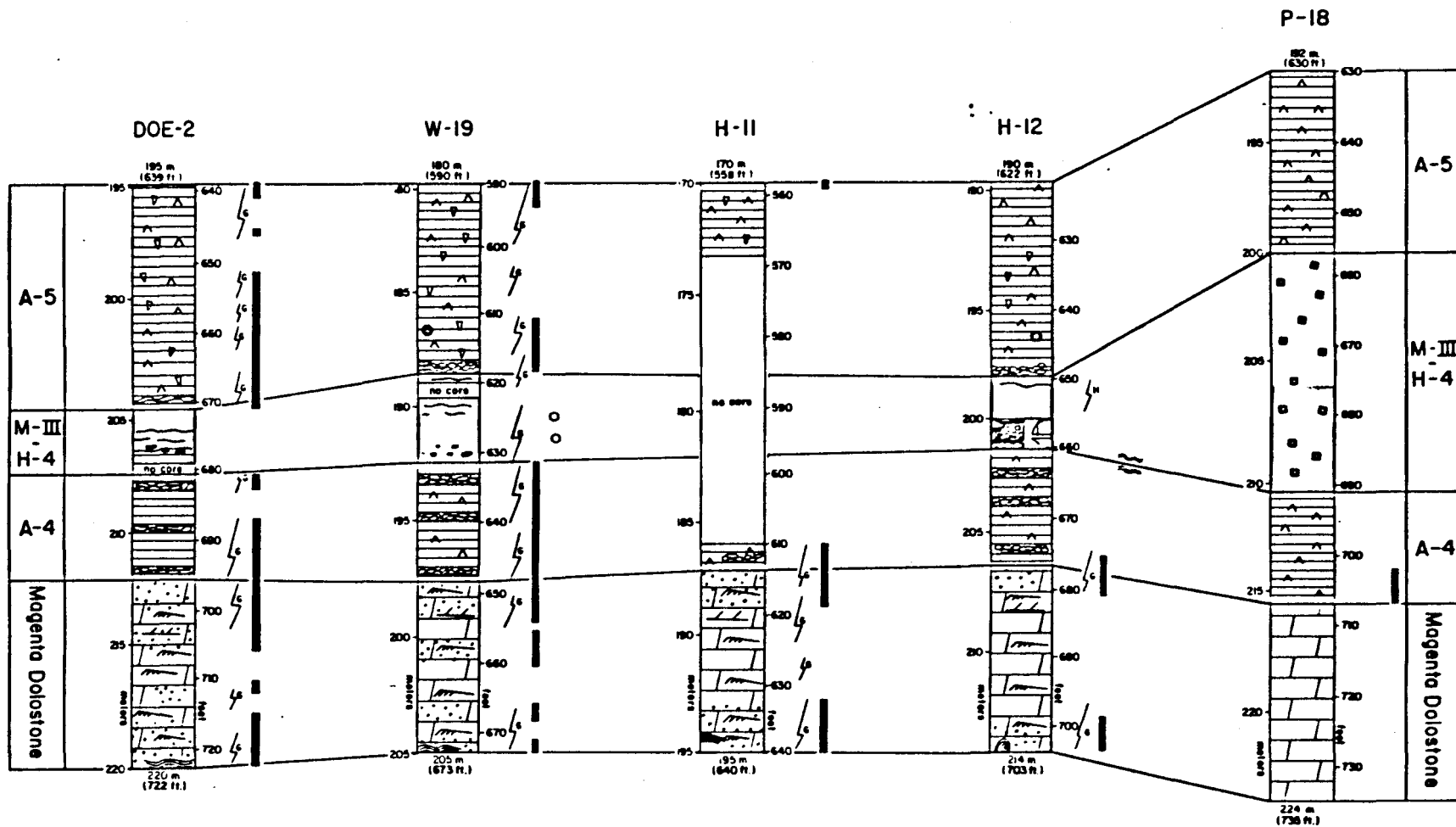


Figure 6(a). Stratigraphic columns-Magenta and Forty-Niner Members, Rustler Formation.  
 (See Fig. 6b for Legend)

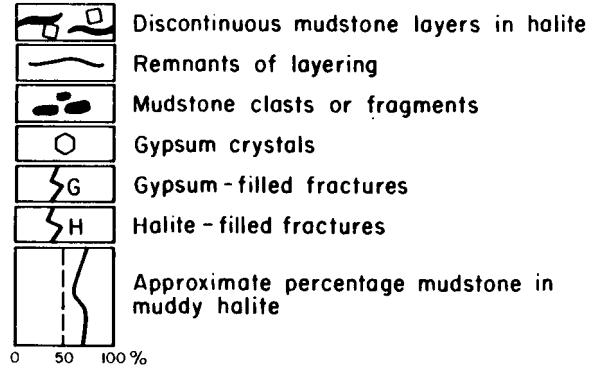
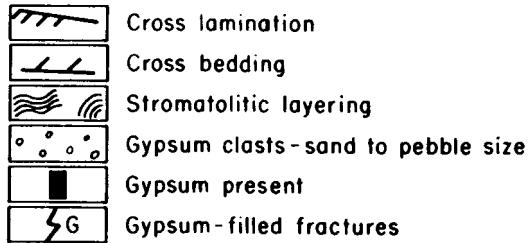
ROCK TYPES



SEDIMENTARY AND DIAGENETIC FEATURES

MAGENTA DOLOSTONE

M·III - H·4



A·4, A·5

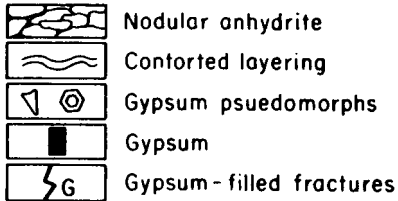


Figure 6(b). Stratigraphic columns-Magenta and Forty-Niner Members, Rustler Formation. (Legend for Fig. 6a)



The basal siliciclastic very fine grained sandstone and mudstone (S-1) displays a systematic vertical variation of sedimentary features in all four cores (Fig. 4). At the base, it is composed of mottled gray-green siltstone to very fine-grained sandstone with patchy preservation of fine scale flat parallel lamination and wavy parallel lamination as well as small scale cross lamination (Photo 1). Burrows of cm-scale size, oval to circular shape in cross section, and variable orientation are common (Photo 1). In core H-12, four layers of dolomitic grainstone, from 5-30 cm in thickness, were identified near the base of the sequence (Fig. 4). These grainstones contain oolites, coated grains, peloids, shells of gastropods, bivalves, brachiopods and bryozoa, and pebbles made of aggregates of dolomitic peloids. Dolomite, anhydrite and halite have replaced all the shell material and may also form void-filling cement.

The upper half of this siliciclastic sequence commonly contains well preserved layering, no fossils and few to no burrows. Sedimentary structures include flat, wavy and contorted lamination, cross lamination and erosionally bounded sets of low angle cross strata, 5 to 15 cm in thickness. The sequence is capped by 1.5 m to 1.8 m of laminated mudstone and sandstone (Photo 2). There, anhydrite is common as nodules and discontinuous laminae. One horizon identified in all cores contains vertical fissures that disrupt layering and which are filled with anhydrite and siliciclastic sediment (Fig. 4, Photo 2).

The siliciclastic sandstone and mudstone sequence (S-1) is interpreted to have been deposited in an open marine embayment. The fossils, especially the bryozoa identified in core H-12, indicate normal marine conditions near the base of the sequence. These sediments record a major marine transgression over the underlying salt-pan-saline mudflat halite of the Salado Forma-

tion. The better preservation of sedimentary structures, the lack of fossils and the sparse burrows higher in the sequence indicate more restricted conditions, probably shallower water with elevated salinities. The uppermost part of the sequence records the final phase of drying of the marine embayment. The fissured horizon is interpreted as a widespread subaerially exposed surface on which prism cracks formed by desiccation. The disrupted/contorted layering near the top of the sequence may record the disruptive effects of ephemeral salt crusts.

Post depositional diagenetic features observed in the S-1 sequence include replacement of carbonate peloids, oolites, and shells by dolomite, anhydrite and halite, fractures filled with halite, and microfaulting (Fig. 4). No features diagnostic of late-stage alteration or dissolution were observed.

The muddy halite of the Lower Member (H-1) contains mudstone, less commonly sandstone, and mm to cm size, subhedral to euhedral cubes of halite (Fig. 4 and Photos 3 and 4). The halite occurs as randomly oriented isolated crystals or as crystalline aggregates. Halite makes up only about 10% of the rock near the base of the sequence. There, well preserved lamination and lenticular thin beds of mudstone and very-fine grained sandstone are found (Fig. 4 and Photo 3). Higher in the sequence, where halite is more abundant (up to about 70% of the rock), the layering is commonly no longer visible and the rock is structureless mudstone-halite (Photo 4). Irregularly shaped pockets and lenses of mudstone, some with concave-up dish structure, may separate crystalline aggregates of halite.

The muddy halite (H-1) is interpreted to have formed in a saline mudflat setting by the mechanism of syndepositional displacive growth of halite at or below the level of a halite saturated

shallow groundwater brine. The siliciclastic sediment was derived from the basin margins and was transported to the center of the basin by episodic floods, by winds, or by a combination of the two. The layering was disturbed later, probably by the intrasediment growth of displacive halite.

The only probable later diagenetic features observed in the H-1 muddy halite are vertically oriented fractures filled with halite. No features diagnostic of late-stage alteration or dissolution are present.

The anhydrite-halite sequence of the Lower Member (A-H-1) is shown in Figure 4 and Photo 5. The anhydrite layers are from 1mm to about 30 cm in thickness, and in core H-12, a bed of anhydrite one meter thick occurs at the base. The anhydrite contains gray to gray-green mud partings that define sub-cm scale lamination. Pseudomorphs of vertically oriented gypsum prisms and randomly oriented equant gypsum crystals (now anhydrite and halite) occur in cores H-12, DOE-2 and W-19. The halite of this sequence is bedded, with laminae of anhydrite (Photo 5) and lenses of mudstone defining layering. The halite contains well preserved primary sedimentary textures, most commonly fluid inclusion-banded chevron and cornet crystals. The upper surfaces of halite layers are commonly truncated and overlain by anhydrite or mudstone.

The anhydrite-halite sequence of the Lower Member is interpreted to have formed in a shallow saline lake - salt pan setting. The rock contains many textures (vertical gypsum pseudomorphs, chevron-cornet halite with syndepositional dissolution truncations) that are identical to those found in modern shallow hypersaline lakes and salt pans (Lowenstein and Hardie, 1985; Hardie, Lowenstein and Spencer, 1985).

The major post depositional modification of the A-H-1 unit is the dehydration of an originally gypsum-rich sediment to anhydrite. No features diagnostic of late-stage alteration or dissolution are present.

The muddy halite (H-2) of the Lower Member is shown in Figure 4 and Photo 6. The halite crystals are commonly subhedral to euhedral, mm to cm size cubes. Isolated crystals of halite or crystalline aggregates separated by mudstone lenses are both present. Discrete layers of halite, from 1 to 5 cm in thickness and composed of vertically directed chevron and cornet crystals, were found in one zone of cores H-12 and DOE-2. The mudstone occurs as discontinuous layers and pockets which, in places, contain internal lamination (Photo 6). Mudstone is also commonly disseminated between and incorporated within halite crystals.

The muddy halite (H-2) is interpreted as a saline mudflat deposit, formed in a manner similar to that described for the muddy halite in H-1. The muddy lenses with internal layering probably formed by infilling depressions of an irregular ephemeral salt crust at the surface.

The only later diagenetic features observed in the H-2 muddy halite are a few halite-filled fractures.

The anhydrite (A-1) of the Lower Member is shown in figure 4 and Photos 7 and 8. Most of the anhydrite is laminated with mm to cm scale layers of anhydrite separated by mudstone containing magnesite. Probable small-scale cross stratification was seen in one zone in all four cores. Pseudomorphs after gypsum (now anhydrite and halite) are common in this interval. The gypsum pseudomorphs are (1) vertically oriented prisms originating from a common depositional surface, (2) large zoned euhedral crystals

up to 10 cm in size and replaced by halite and anhydrite and (3) sand sized equant, unoriented gypsum crystals (Photo 7).

The top of the sequence in all four cores contains about 30 cm of anhydrite and gypsum (Photo 8). Features observed there include (1) rounded to angular fragments ("islands") of anhydrite in massive gypsum, (2) subhorizontal layers of gypsum, (3) massive gypsum, (4) subhorizontal gypsum-filled fractures, and at the top, (5) angular fragments of gypsum or anhydrite surrounded by brown mudstone (Photo 8).

The anhydrite of the Lower Member is interpreted to have formed in a shallow hypersaline lagoon saturated with respect to gypsum. The original sediment was probably gypsum and minor carbonate mud. The vertically oriented gypsum pseudomorphs and probable cross lamination indicate shallow water depths. The major post-depositional diagenetic feature of the A-1 anhydrite is the dehydration of gypsum to anhydrite and minor pseudomorphous replacement of some gypsum by halite.

The upper part (about 30 cm) of the A-1 anhydrite is interpreted to have undergone late-stage alteration involving hydration of anhydrite to gypsum, and, in one core (DOE-2), the probable dissolution of halite that once formed pseudomorphs after gypsum. The evidence and mechanisms of this late-stage alteration are discussed below.

The uppermost rock type of the Lower Member in the four cores examined is mudstone (M-I) (Fig. 4 and Photos 8 and 9). The mudstone is poorly lithified and "crumbly", and predominantly structureless. Some remnants of highly contorted and folded layering were observed. Additional features include (1) round to angular cm-size fragments or clumps of mudstone, (2) angular

fragments of gypsum or anhydrite, up to 5 cm in diameter, surrounded by mudstone. (3) isolated euhedral gypsum crystals and gypsum crystal rosettes. (4) disseminated calcite (identified using 10% HCl solution), and (5) numerous fractures filled with fibrous gypsum up to 2 cm thick and oriented at varying angles from horizontal to 60° from the horizontal (Photo 9). The top of this unit grades into laminated dark gray mudstone with well preserved wavy to flat parallel lamination.

The environment of deposition of the mudstone (I) is difficult to assess from examination of the four cores because, besides the contorted remnants of layering, there are no unequivocal primary sedimentary structures preserved. This rock is interpreted to have undergone significant late diagenetic alteration (see below). In core P-18 to the east, halite with polyhalite and brown mudstone is interpreted to occupy the same stratigraphic position as the mudstone (I) (Fig. 4) (Jones, 1978; Snyder, 1985).

#### CULEBRA DOLOMITE MEMBER

The Culebra Dolomite Member is a tan to gray colored dolostone with minor quartz silt (Fig. 5 and Photos 10 and 11). The rock is predominantly structureless, although vague layering, on a scale of 1-5 cm, is seen in places. Well preserved mm-scale lamination is present at the base of the unit. The top of the Culebra Member, about 30 cm in thickness, is finely laminated and the unit is capped by a brown to black laminite with sub-mm scale, black organic-rich and tan carbonate-rich layers. One common feature of the Culebra Dolomite is the large number of nodular masses and open vugs from a mm to greater than 10 cm in diameter. They are roughly spherical to ellipsoidal in shape and are in sharp contact with the surrounding dolostone. In

core H-12, the vugs are open or filled with (1) a core of anhydrite laths and a rim of gypsum (Photo 10) or (2) gypsum. In the other 3 cores, most of the vugs are open but some are entirely filled with coarse gypsum crystals (Fig. 5).

The Culebra Dolomite is intensely fractured which has led to generally poor core recovery. Fractures are oriented in all directions, from the horizontal to the vertical and they are open or filled with gypsum (Fig. 5 and Photo 11). The gypsum fracture filling is either fibrous or occurs as coarse sparry crystals. Also present are pockets of dolostone pebbles cemented by gypsum. They consist of unsorted, angular fragments of dolostone which may display "fitted" textures.

The Culebra Dolomite was probably originally composed of carbonate mud. The dolomite is very finely crystalline with crystal sizes of about  $10\mu$ . There is little textural evidence of a precursor carbonate nor were any fossils or burrows identified. Features indicating subaerial exposure were not found. Taken together, the textures of the Culebra suggest that it was deposited as carbonate mud in an aerially extensive lagoon with restricted circulation and slightly elevated salinities. Sometime after deposition, the carbonate was replaced by well ordered dolomite. The origin of the nodular masses and vugs is uncertain, but similar features, made of anhydrite, have been interpreted by Clark (1980) as concretions in the Zechstein Formation of Western Europe. Whatever their origin, the nodular masses of the Culebra are believed to have once been completely filled with anhydrite. Anhydrite is still found in the cores of some of the larger nodules of core H-12 (Photo 10). These anhydrite nodules are rimmed by gypsum, interpreted as a hydration replacement mineral formed during late stage alteration. In the other 3 cores, it is interpreted that all the anhydrite

has been converted to gypsum or has been dissolved. Other evidence for late stage alteration is the intense fracturing and the filling of some fractures with gypsum. The pockets of angular dolostone pebbles cemented by gypsum are interpreted to have formed by late stage in-situ brecciation. The late stage alteration of the Culebra Dolomite Member will be discussed later.

#### TAMARISK MEMBER

The Tamarisk Member of the Rustler Formation contains, in ascending order, anhydrite (A-2); mudstone (M-II) and in core H-12, halite-muddy halite (M-II - H-3); and anhydrite (A-3) (Fig. 5).

The anhydrite (A-2) of the Tamarisk Member contains a variety of textures and fabrics including (1) laminated anhydrite with mm to cm scale anhydrite layers separated by muddy partings, (2) nodules of anhydrite surrounded by gray-green mudstone, and (3) structureless anhydrite. Contorted layering was seen in cores H-12 and DOE-2 (Fig. 5). Gypsum pseudomorphs were observed in cores H-12, DOE-2 and H-11. The pseudomorphs are (1) sub cm-size vertically oriented prisms (now anhydrite), (2) sub-cm size randomly oriented equant euhedral crystals outlined by mudstone. (now anhydrite), and (3) large zoned crystals, up to 5 cm in size and now composed of halite and anhydrite (core H-12).

In core H-12 gypsum occurs in the bottom 30 cm of this unit and sub horizontal gypsum-filled fractures occur in the lowest 60 cm (Fig. 5). The top of the sequence in H-12 contains 15 cm of bedded halite and anhydrite, which is overlain by halite. Core H-11 contains laminated gypsum and subhorizontal gypsum-filled fractures in the lowest 60 cm of the sequence (Fig. 5). In core



DOE-2, gypsum occurs in the bottom 30 cm, the middle and the top 60 cm of the sequence and gypsum-filled fractures are found throughout. The A-2 anhydrite of the Tamarisk Member is not present in the WIPP-19 core.

The sedimentary setting in which the anhydrite (A-2) was deposited cannot be established with certainty because of the limited number of sedimentary structures. However, the identification of gypsum pseudomorphs indicates that the original sediment was composed of gypsum and mud. The gypsum has been dehydrated to anhydrite sometime after deposition. The rock contains evidence for late-stage alteration of anhydrite to gypsum in the bottom of cores H-11 and H-12 and the bottom, middle and top of core DOE-2. The alteration process has involved rehydration of anhydrite to gypsum and fracturing, with gypsum commonly filling the fractures. The entire sequence is absent in core W-19. Based on the detailed correlation of this anhydrite across the study area, the A-2 anhydrite in core W-19 is interpreted to have been removed by late-stage dissolution processes (see below).

The halite-muddy halite rock of the Tamarisk Member (H-3) is only present in core H-12 (Fig. 5 and Photo 12). The bottom of the sequence predominantly consists of clear halite crystals of about cm size. Fluid inclusion-banded chevron/cornet halite was identified in some intervals. Small amounts (less than 5%) of gray-green to brown mud and anhydrite occur interstitial to halite crystals and as discontinuous laminae (Photo 12). The upper half of the halite sequence in core H-12 contains greater amounts of mud as discontinuous lenses and pods and contorted thin beds (Fig. 5). In thin section (core H-12 at 236.2 m or 775 ft), the halite contains primary textures including fluid inclusion banded chevron and cornet crystals, some with syndepositional solution truncations.

In the other three cores (H-11, W-19 and DOE-2), no halite was identified in this interval. The rock is predominately structureless brown mudstone (II), which is much thinner than the halite sequence of core H-12 (Fig. 5, and Photos 13, 14, 15). Where sedimentary layering was observed, it is folded or tilted at an angle of 20 to 30° from the horizontal. The rock, in places, contains mm to cm size, unsorted, angular fragments of gypsum or anhydrite and angular to rounded mudclasts all floating in a brown mudstone matrix (Photo 14). Gypsum is common in this sequence as scattered crystals and crystal rosettes (Photo 13) and as a fracture filling (Photo 15). Disseminated calcite was detected with 10% HCL solution.

The halite-muddy halite (H-3) of the Tamarisk Member has not been studied in great detail. Based on core examination and one thin section (H-12, 236.2m; 775 ft), the halite probably formed in a salt pan-saline mudflat setting. Shallow water conditions are indicated by the presence of primary, fluid inclusion banded halite with syndepositional solution truncations (see Lowenstein and Hardie, 1985). The mudstone (M-II) at the same stratigraphic position in cores H-11, W-19 and DOE-2 contains few primary sedimentary structures so interpretations of depositional environments are difficult. This sequence is interpreted to have suffered extensive late-stage alteration, which will be discussed in a later section.

The anhydrite (A-3) of the Tamarisk Member is shown in Figure 5 and Photos 16 and 17. In general, the sedimentary structures present in this anhydrite can be correlated in all four cores across the study area. The rock is for the most part laminated with cm-scale anhydrite layers separated by dolomitic (?) mudstone. Gypsum pseudomorphs are abundant as (1) sub-vertically oriented prisms (Photo 17) and (2) randomly oriented equant crystals surrounded by mudstone.

The upper half of the sequence contains few gypsum pseudomorphs and the layering is disrupted to produce a nodular or "lumpy" texture. Dolostone layers are common as lenses and thin beds and they become most abundant near the top of the unit where it grades into the overlying Magenta Dolostone. In all four cores, the base of the A-3 anhydrite contains contorted layers of laminated anhydrite and gray-green mudstone and clasts of anhydrite in a mudstone matrix. In core H-11, the bottom 1.8 m contains (1) unsorted brecciated fragments of anhydrite (Photo 16), some with internal layering showing that the clasts have been rotated and deformed, and (2) folded and deformed anhydrite-mudstone laminae. In core W-19, the basal 30 cm is brecciated and the layering in the bottom 6 m or so dips at angles of 20-30° from the horizontal. A small fault was observed at 216.4 m. The bottom 90 cm of the DOE-2 core also contains folded and contorted laminae and brecciated fragments, which are cemented by gypsum spar. Gypsum is present in the top 60 cm of cores H-11 and H-12, in the bottom 6.7 m and top 3.7 m of core W-19 and the bottom 11.3 m and top 0.6 m of core DOE-2 (Fig. 5). Gypsum-filled fractures occur in about the same stratigraphic position as the gypsum in all four cores (see Fig. 5).

The A-3 anhydrite is interpreted to have been originally composed of gypsum and carbonate-rich mud. The gypsum pseudomorphs, predominantly in the lower half of the unit, indicate deposition in a shallow lagoon at gypsum saturation. Sometime after deposition, all the gypsum has been converted to anhydrite and all the carbonate mud has been dolomitized. There is abundant evidence that the A-3 anhydrite has suffered late-stage alteration. The basal breccia and the contorted and tilted layering are all interpreted as slump or collapse features. The presence of gypsum and gypsum-filled fractures, which show a progressive increase in abundance across the study area (Fig. 5)

are interpreted to have formed by late-stage fracturing, cementation and rehydration of anhydrite. Petrographic study of the gypsum-bearing section of the DOE-2 core shows that gypsum crystals crosscut the primary sedimentary textures of the rock. Compared to the same stratigraphic interval in core H-12, the DOE-2 core shows much poorer preservation of primary sedimentary textures. The alteration process will be discussed in more detail below.

The Magenta Dolomite Member of the Rustler Formation is shown in Figure 6 and Photos 18, 19, 20 and 21. The unit is virtually identical across the study area. It is composed of dolomite, (as anhedral to subhedral crystals that may outline very-fine peloidal sand), gypsum, minor quartz silt and very fine sand and traces of anhydrite. Notable sedimentary structures include (1) dolomitic laminites with organic partings and probable gypsum pseudomorphs (Photo 18) and a dolostone stromatolite, both at the base of the Magenta (Photo 19), common wavy laminae to thin beds that are internally massive or cross laminated (Photo 20), scour and fill and cross bedding (Photo 21). Gypsum is common, especially near the top and bottom of the unit, as sand size clasts and pebble-sized spherical to ellipsoidal shaped masses. Thin sections from cores H-11 and W-19 show that the gypsum is commonly a coarse spar. Some microcrystalline laths of anhydrite are commonly found in the cores of the gypsum nodular masses and clasts. Small scale faulting and fracturing is common, with most fractures filled with satin spar gypsum. The intensity of fracturing increases across the study area (see Fig. 6).

The Magenta Dolostone Member was probably originally deposited as peloidal carbonate sand and mud, quartz silt and gypsum crystal sand. The lack of fossils and the presence of gypsum

sand clasts and a primary gypsum crystal layer near the base suggests that the waters were too saline to allow organisms to survive. There is no evidence for subaerial exposure. The abundance of current-formed sedimentary structures suggests that the predominant environment of deposition was a shallow marine embayment. Following deposition, all the carbonate was converted to dolomite and all the gypsum was converted to anhydrite. Evidence for late stage alteration includes fractures filled with gypsum and rehydration of the anhydrite sand clasts and nodules to gypsum (see below).

#### THE FORTY NINER MEMBER

The Forty Niner Member of the Rustler Formation contains, from bottom to top, anhydrite (A-4); mudstone (III), which in core H-12 contains muddy halite (H-4); and anhydrite (A-5) (Fig. 6).

The anhydrite (A-4) of the Forty Niner Member chiefly consists of bedded nodular anhydrite. The anhydrite nodules are cm-scale in size and commonly flattened. In core H-12, gypsum and gypsum-filled fractures occur in the bottom 30cm. In the other cores, gypsum and gypsum-filled fractures are found throughout the sequence.

There are no primary sedimentary structures in this anhydrite that are diagnostic of any particular depositional environment. The gypsum and gypsum-filled fractures, especially common in DOE-2 and W-19, are interpreted as late-stage alteration features.

The mudstone-muddy halite (H-4) of the Forty Niner Member is only found in core H-12 (Fig. 6). The base of the sequence is a gray-green mudstone with vague contorted lamination. Immediate-

ly above it is a sequence of muddy halite. The halite consists of mm to cm size crystals and crystalline aggregates with incorporated mud. Mudstone pockets and lenses may separate crystalline aggregates of halite. A thin section of this halite contains both fluid-inclusion banded chevron halite and clear, mud incorporative displacive halite. The sequence is capped by red-brown mudstone, predominantly structureless but with traces of layering (Fig. 6).

The same stratigraphic interval in the W-19 and DOE-2 cores consists of mudstone (M-III). It is predominantly structureless with vague remnants of contorted layering. Pebble sized clasts of mudstone and gypsum occur at the base of the unit in DOE-2. Scattered gypsum crystals and gypsum-filled fractures were seen in the W-19 core.

The mudstone-muddy halite of the H-12 core is interpreted as a salt pan-saline mudflat deposit, based on the chevron halite and displacive halite textures observed in cores and thin section. In cores W-19 and DOE-2, few sedimentary structures are preserved so interpretation is difficult. The gypsum fragments, gypsum crystals, and gypsum-filled fractures are interpreted as late-stage alteration features (see below).

The uppermost anhydrite (A-5) of the Forty Niner Member is shown in Figure 6 and Photos 22, 23 and 24. The anhydrite is commonly laminated and contains abundant pseudomorphs of gypsum that have been replaced by anhydrite. The gypsum pseudomorphs are commonly mm to cm in size and vertically aligned. Mud partings may form drapes over these pseudomorphs. Other types of gypsum pseudomorphs are present including zoned equant crystals.

The anhydrite (A-5) of the Forty Niner Member is similar to the laminated anhydrite described by Lowenstein (1982) in the Salado Formation. The primary sediment was carbonate mud and gypsum formed in a shallow lagoon setting. The growth of gypsum on the lagoon floor as vertically-oriented prisms was interrupted by the deposition of thin carbonate-rich mud layers. Some of the gypsum may have been reworked into detrital crystal sand layers.

There is firm evidence that this anhydrite has suffered late-stage alteration. The H-12 sequence is composed entirely of anhydrite although the cap of the sequence was not studied. Core H-11 contains gypsum in the top 30 cm at the Rustler-Dewey Lake Formation Contact. W-19 and DOE-2 contain gypsum fracture fillings and gypsum over much of the sequence. All the gypsum is interpreted to have formed during late stage alteration by replacement of anhydrite (Photos 22, 23 and 24) and by precipitation in fractures. This alteration process will be discussed in the next section.

## CRITERIA FOR RECOGNIZING LATE STAGE ALTERATION

Features interpreted to have been produced by late-stage alteration have been observed in all four cores of the Rustler Formation in the study area. This alteration has occurred to varying degrees in the top of the Lower Member (A-1 anhydrite and Mudstone I), the Culebra Dolomite Member, the Tamarisk Member (A-2 anhydrite, Mudstone II and A-3 anhydrite), the Magenta Dolomite Member, and the Forty Niner Member (A-4 anhydrite, Mudstone III and A-5 anhydrite) (see Figs. 4, 5 and 6). The alteration has involved physical processes such as brecciation, slumping, fracturing and faulting and chemical processes such as rehydration of anhydrite to gypsum, gypsum precipitation and dissolution of halite, anhydrite and gypsum.

Two assumptions that have led to the above interpretations are first addressed. First, the Rustler Formation occupies an enormous area, greater than 100,000 km<sup>2</sup>, so it may be properly called a "saline giant". All the rock types observed in the study area are interpreted to have originally been deposited in shallow water to subaerially exposed settings. Such shallow water facies normally record with great sensitivity the environments in which they were deposited. Indeed, in the four cores studied, stratigraphic correlations are readily made. Furthermore, many of the stratigraphic units contain a detailed internal stratigraphy that can be easily matched from core to core (see Figs. 4, 5 and 6; S-1, H-1, A-H-1, and A-1 units of the Lower Member; Culebra Member; A-2 and A-3 anhydrite of the Tamarisk Member; the Magenta Member; and the A-4 and A-5 anhydrites of the Forty Niner Member). Therefore, across the study area, major facies changes are not observed. This area is only a small part of the Rustler Formation, which as a whole, was probably deposited in a low-relief basin (Fig. 1).



Therefore, the detailed stratigraphic correlation is not surprising. Abrupt thinning of stratigraphic units or changes in rock types across the study area should then sound a warning that some post-depositional processes may be at work.

The second assumption is that sometime after deposition, most, if not all, of the  $\text{CaSO}_4$  in the Rustler Formation was anhydrite. The abundant pseudomorphs of gypsum, now composed of anhydrite, indicate that an originally gypsum-rich sediment has since been converted to anhydrite. This assumption is backed by evidence from many other ancient evaporites where primary gypsum has been wholly converted to anhydrite upon burial. Therefore, the gypsum now present in the Rustler is interpreted to have formed as a rehydration replacement of anhydrite or as a void filling cement, or fracture filling, the three of which are commonly associated. There is abundant evidence indicating that the formation of gypsum as one of the above textures has been the last process that has operated in the Rustler Formation. This evidence includes (1) gypsum-filled fractures that crosscut all other sedimentary features, (2) gypsum crystals with remnants of anhydrite in the cores of nodules and clasts, and gypsum rims around anhydrite nodules (Culebra Dolomite), and (3) gypsum-cemented breccias. Thus, where the gypsum of the Rustler Formation forms anything other than a void-filling, it is interpreted to have undergone the transformation sequence of dehydration of gypsum to anhydrite (upon burial) and rehydration of anhydrite to gypsum (upon exhumation). Such changes should result in the loss of primary sedimentary structures compared to rocks still composed of anhydrite and in general this is true. In such "gypsified" rocks, the gypsum crystals may crosscut the original gypsum pseudomorph boundaries, which confirms that the gypsum is a later alteration product.

The presence of gypsum in the Rustler Formation therefore serves as a general indicator of late stage alteration (see Figs. 4, 5 and 6). In all zones identified as altered in the study area, gypsum is present. Waters capable of directly precipitating gypsum and rehydrating anhydrite to gypsum on a large scale are not likely to be connate evaporite formation waters, but were probably introduced into the rock at some later time. In the Rustler Formation, the most likely candidate for an introduced "alien" water is groundwater. The present-day Rustler Formation waters (in the Culebra and Magenta Dolomites) are for the most part "dilute" and probably meteoric in origin. These waters have not migrated from the evaporites within or below the Rustler Formation. The chemistry of present-day Rustler Formation waters will be further discussed below.

#### Evidence for late-stage chemical alteration

The textural features in the Rustler Formation interpreted to have formed during late stage chemical alteration by the introduction of alien waters include (1) precipitation of gypsum as void-filling cement, breccia cement and fracture filling (Figs. 4, 5 and 6 and Photos 8, 9, 11, 15, 19), (2) replacement of anhydrite by gypsum by rehydration (Figs. 4, 5 and 6 and Photos 8, 10, 22, 23, 24), (3) precipitation of euhedral gypsum crystals and gypsum crystal rosettes (Figs. 4, 5 and 6 and Photo 13), (4) dissolution of gypsum and anhydrite (open vugs in Culebra and Magenta Dolomite Members, Photos 10 and 11) and (5) precipitation of calcite (Figs. 4, 5 and 6).

#### Evidence for late-stage physical alteration

The physical features interpreted to have been produced by late stage alteration are commonly associated with those produced by chemical alteration. These include (1) fractures and small

scale faults (Photo 11) (2) tilted beds, (3) contorted and folded layering, (4) brecciation, with angular clasts of dolostone or anhydrite/gypsum which may be cemented with gypsum. (The breccias may display "fitted textures" demonstrating an in situ origin (Photo 16); other breccias contain unsorted angular fragments of anhydrite with internal layering that show that the fragments have been rotated and deformed), (5) Non-clast supported conglomerate with cm size, angular and unsorted fragments of gypsum or anhydrite or round to angular clasts of mudstone in a mudstone matrix (Photo 14). Taken alone, some of these features may not be unequivocal indicators of later stage alteration, especially 3 above. But these features are commonly associated with one another and with features diagnostic of late-stage chemical alteration. Moreover, primary sedimentary structures in these stratigraphic intervals may be strongly overprinted or absent.

The intensity of these alteration features may, in some cases, change progressively from least altered (core H-12) to most altered (cores DOE-2 and W-19) across the study area. For example, in the Tamarisk Member of core H-12, alteration to gypsum together with gypsum filled fractures are seen only in the bottom 60 cm of the A-2 anhydrite and the top meter or so of the A-3 anhydrite. In comparison, gypsum filled fractures and replacement gypsum are found over much of the A-2 and A-3 anhydrites of the DOE-2 core (see Fig. 5). Other intervals in which such lateral variations in alteration occur include the Culebra Dolomite Member in which remnants of anhydrite are still found in core H-12 while in cores DOE-2 and W-19 most vugs are open or filled with gypsum (Fig. 5). In the Forty-Niner Member (anhydrites A-4 and A-5) and the Magenta Dolomite Member the same pattern of increased fracturing and gypsification is seen between cores H-12 and DOE-2 (see Fig. 6). In contrast,

the pattern of alteration across the study area in the Lower Member of the Rustler Formation (top 30 cm of A-1 anhydrite and Mudstone I) is uniform (Fig. 4).

## DISSOLUTION OF EVAPORITES IN THE RUSTLER FORMATION

The question of whether widespread dissolution of evaporites has occurred in the Rustler Formation may not be addressed with direct observations: the dissolved species produced by solution are removed from the site of reaction. Therefore, the identification of evaporite dissolution and the amount of dissolution is interpretive. In this detailed study, interpretations on dissolution are based on two observations. First, the lack of significant lateral changes in the primary sediments and inferred depositional settings of the Rustler Formation in the area of study. In this area, which represents less than about 0.05% of the total area of deposition of the Rustler Formation, detailed stratigraphic correlations based on sedimentary structures and textures indicate overall uniformity of depositional setting. Second, the identification of physical and chemical alteration features, which, based on crosscutting relations, represent the last processes which have operated on these rocks.

If the two observations outlined above are correct, then stratigraphic intervals in which widespread dissolution has occurred may display abrupt lateral changes in rock type and rock thickness. Such intervals must also contain some or all of the features diagnostic of late-stage physical and chemical rock alteration by relatively dilute, alien waters (see discussion above).

For the four cores examined, the following stratigraphic intervals are interpreted to have undergone significant late-stage evaporite dissolution: (1) Halite from the Mudstone I (M-I) interval of the Lower Member in all four cores (Fig. 4), (2) the A-2 anhydrite of the Tamarisk Member in Core W-19, (Fig. 5), (3) Halite from Mudstone II (M-II) of the Tamarisk Member in cores

H-11, W-19 and DOE-2 (Fig. 5). In addition, halite may have been removed from Mudstone III (M-III) of the Forty-Niner Member in cores W-19 and DOE-2, but the evidence is equivocal. The amount of possible halite dissolution in this interval however is small (see Fig. 6).

The following generalizations may be made for the stratigraphic intervals in which widespread dissolution has been interpreted (see Figs. 4, 5 and 6 and earlier discussion).

- (1) Late-stage physical and chemical alteration features are present.
- (2) Changes in rock type (mineralogy) and rock thickness occur over short lateral distances.
- (3) Dissolution zones may be located immediately above (A-2 anhydrite, W-19 core) or below (M-I mudstone) present day aquifers.

In addition, stratigraphic intervals immediately above and below the inferred dissolution zones exhibit the following:

(4) Late-stage physical and chemical alteration features, especially near the contacts with the inferred dissolution zone (top of A-1 anhydrite and Culebra Dolomite, Fig. 4 and 5; Culebra Dolomite and A-3 anhydrite, Fig. 5; A-2 anhydrite and A-3 anhydrite, Fig. 5; A-4 anhydrite and A-5 anhydrite, Fig. 6). These surrounding stratigraphic intervals are not heavily dissolved because they are predominantly composed of dolostone and anhydrite which are far less soluble than halite, the mineral interpreted to have been removed in all but one of the dissolution zones. These relations are best seen for the rocks above the M-

II mudstone, in which, based on stratigraphic correlation, the largest amount of halite has been dissolved (Fig. 5). The A-3 anhydrite directly above the inferred dissolution zone contains abundant gypsum-filled fractures, breccias with rotated fragments, gypsified anhydrite and tilted and contorted beds (Cores DOE-2, W-19, and H-11). Such features are interpreted to have formed by mechanical slumping and collapse over the underlying dissolved halite interval and by chemical alteration by migrating alien waters.

(5) No lateral changes in thickness, rock type or sedimentary structures. Though the rocks above and below inferred dissolution zones are chemically and physically altered, they still contain abundant sedimentary structures and an internal stratigraphy that can easily be matched from core to core. These surrounding intervals are also about the same thickness across the study area. (An exception, of course, is the lateral change from anhydrite to gypsum, interpreted as a late-stage rehydration process.)

#### Possibility of Present-Day Dissolution

The question of whether active dissolution is presently occurring in the Rustler Formation in the study area may be addressed through study of the chemical composition of Rustler Formation waters. The chemical composition of these waters is presented in Ramey (1985) for three stratigraphic intervals: the Rustler-Salado contact, the Culebra Dolomite and the Magenta Dolomite. Water analyses from 11 wells located within 5 km of the four borehole cores were selected for detailed study (H-1, H-2, H-3, H-4, H-5, H-6, P-14, P-15, P-17, P-18, and W-30).

The contact between the Salado Formation and the Rustler Formation does not appear to have undergone any late-stage

alteration for the three cores examined. The water analyses from locations near the cores studied confirm this interpretation. Nearly all the waters from this zone are halite saturated brines with total dissolved solids greater than 300,000 mg/l. (Exceptions are wells P-15 and P-17 both located to the west of the studied cores). These brines are chloride-rich with significant concentrations of Na<sup>+</sup>, Mg<sup>+2</sup>, K<sup>+</sup> and Ca<sup>+2</sup>. Such brine compositions could not be produced by simple dissolution of halite, nor are they now capable of dissolving significant quantities of evaporites.

Compared to the waters at the Salado-Rustler contact, the formation waters in the Culebra Dolomite are quite dilute. Of the eleven wells in the vicinity of the borehole cores studied, four contain waters with 30,000 mg/l or less dissolved solids, and the most concentrated waters (well H-5) contain only 144,000 mg/l total dissolved solids. Despite the uncertainty associated with saturation calculations for high TDS waters, calculations indicate that all these waters are undersaturated with respect to halite ( $\log IAP_{NaCl}/K_{Halite} = -1.1$  to  $-3.9$ ). Moreover, eight of the eleven wells contain waters undersaturated with respect to gypsum ( $\log IAP/K = -0.016$  to  $-1.48$ ) and three of the waters (H-1, H-2, H-3) are slightly supersaturated ( $\log IAP/K = +0.071$  to  $+0.084$  or  $IAP/K < 1.22$ ). The Culebra Formation waters are NaCl dominated with subordinate Ca and SO<sub>4</sub>. These waters, in terms of chemical composition and concentration of dissolved species, would be ideal to produce the types of alteration features that are observed within, above and below the Culebra Dolostone Member. Those undersaturated with respect to gypsum may dissolve gypsum, leaving the numerous open vugs observed in the Culebra Dolomite. Those waters supersaturated with respect to gypsum may precipitate gypsum as cement and fracture filling. Leakage of these waters into the underlying rocks may produce



widespread dissolution of halite as has been interpreted to have occurred in the underlying M-I mudstone. Interestingly, the one well with known halite below the Culebra Dolomite (P-18) contains relatively high total dissolved solids (118,000 mg/l), indicating the possibility of present-day dissolution. Were these waters to leak into the M-II mudstone, just 6 m above the top of the Culebra Dolomite, then widespread dissolution of halite may occur there, as has been interpreted (Fig. 5). Finally, this type of water may have dissolved the A-2 anhydrite directly above the Culebra Dolomite (Core W-19), given a large enough water volume. The significance of the water analyses is that the Culebra waters are relatively dilute and are alien waters introduced into the rock. Their compositions are such that they may have been responsible and indeed may still be responsible for dissolution and alteration of evaporites within, above and below the Culebra Dolomite.

The waters from the Magenta Dolomite are even more dilute than those of the Culebra Dolomite, in the vicinity of the borehole cores studied (total dissolved solids: 5,700 to 30,000 mg/l). They are Na-SO<sub>4</sub>-Cl waters for the most part, with subordinate calcium. These waters are also highly undersaturated with respect to halite ( $\log \text{IAP/K} = -1.8$  to  $-4.5$ ). Of the seven well waters analyzed within 5 km of the cores studied, five are at or slightly above gypsum saturation ( $\log \text{IAP/K} = +0.004$  to  $+0.664$ ) and two are undersaturated with respect to gypsum ( $\log \text{IAP/K} = -0.255$  and  $-0.383$ ). These waters are not connate evaporite waters nor have they ever come into contact and dissolved significant quantities of halite. They are probably meteoric in origin and have migrated from the surface. Such waters would have the capacity to dissolve large amounts of halite, but there is no halite present stratigraphically directly above or below the Magenta in this area. The waters supersaturated with gypsum

could certainly be responsible for the abundant fractures filled with gypsum and for the gypsified anhydrite found within the Magenta Dolomite and within the surrounding A-3 and A-4 anhydrites (Fig. 5 and 6).

## REFERENCES

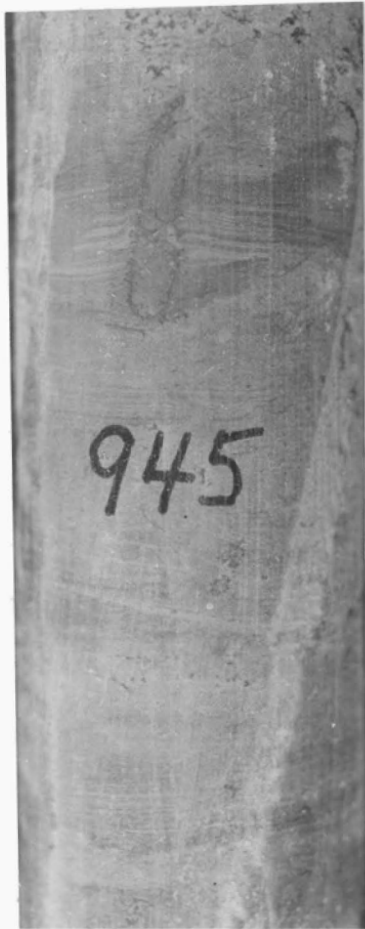
- Bachman, G.O., 1984. Regional geology of Ochoan evaporites, northern part of Delaware Basin: N.M. Bureau of Mines and Min. Res. cir. 184, 22p.
- Chaturvedi, L. and Channell, J.K., 1985. The Rustler Formation as a transport medium for contaminated groundwater: EEG-32, DOE/AL/10752-32, 84p. + Appendices.
- Chaturvedi, L., and Rehfeldt, K. 1984, Groundwater occurrence and the dissolution of salt at the WIPP radioactive waste repository site: Trans. American Geophysical Union (EOS), v. 65, no. 31, p. 457-459.
- Clark, D. N., 1980, The diagenesis of Zechstein carbonate sediments: In: The Zechstein Basin with Emphasis on Carbonate Sequences (Ed. By H. Fuchtbauer and T. Peryt), Contributions to Sedimentology 9, E. Schweizerbart'sche Verlagsbuchhandlung, Stuttgart, p. 167-203.
- Hardie, L. A., Lowenstein, T. K., and Spencer, R. J., 1985, The problem of distinguishing between primary and secondary features in evaporites: In Sixth International Symposium on Salt (Ed. by B. C. Schreiber), p. 11-39, Toronto, Canada, May 1983, Salt Institute, Alexandria, VA.
- Hills, J. M., 1942, Rhythm of Permian seas--a paleogeographic study: Amer. Assoc. Petrol. Geol. Bull., v. 26, p. 217-255.
- Hills, J. M., 1972, Late Paleozoic sedimentation in West Texas Permian Basin: Amer. Assoc. Petrol. Geol. Bull., v. 56, p. 2303-2322.
- Holt, R. M. and Powers, D. W., 1984, Geotechnical activities in the Waste Handling Shaft, WIPP Project, S. E. New Mexico: U. S. Dept. of Energy, WIPP WTSD-TME 038, Var. p.
- Jones, C. L., 1978, Test drilling for potash resources: Waste Isolation Pilot Plant site, Eddy County, N.M.: U. S. Geol. Survey Open File Rpt. 78-592, 2 vols. 431 p.
- Lambert, S. J., 1983, Dissolution of evaporites in and around the Delaware Basin, southeastern N.M.: Sandia National Lab. Report, SAND 82-01, 96 p.

- Lowenstein, T. K., 1982, Primary features in a potash evaporite deposit, the Permian Salado Formation of West Texas and New Mexico: In: *Depositional and Diagenetic Spectra of Evaporites--A Core Workshop* (Ed. by C. R. Handford, R. G. Loucks and G. R. Davies), p. 276-304, SEPM Core Workshop No. 3, Calgary, Canada, 1982.
- Lowenstein, T. K., and Hardie, L. A., 1985, Criteria for the recognition of salt-pan evaporites: *Sedimentology*, v. 32, p. 627-644.
- Mercer, J. W., 1983, Geohydrology of the proposed Waste Isolation Pilot Plant site, Los Medanos Area, southeastern New Mexico: U. S. Geol. Survey, Water-Resources Investigations Report 83-4016, 113p.
- Page, L. R., and Adams, J. E., 1940, Stratigraphy, Eastern Midland Basin, Texas: *Am. Assoc. Petrol. Geol. Bull.*, v. 24, p. 52-64.
- Powers, D. W., Lambert, S. J., Shaffer, S. E., Hill, L. R. and Weart, W. D. (eds.), 1978, Geological Characterization Report, Waste Isolation Pilot Plant Site, Southeastern New Mexico: Sandia National Lab. Report, SAND 78-1596, 2 vols.
- Powers, D. W. and Holt, R. M., 1984, Depositional environments and dissolution in the Rustler Formation (Permian), southeastern New Mexico: (Abs.) *Geol. Soc. Amer.*, 97th Annual Meeting Abstracts with Program, v. 16, no. 6, p. 627.
- Ramey, D. S., 1985, Chemistry of Rustler Fluids: Environmental Evaluation Group Report EEG-31, 61 p.
- Snyder, R. P., 1985, Dissolution of halite and gypsum, and hydration of anhydrite to gypsum, Rustler Formation, in the vicinity of the Waste Isolation Pilot Plant, southeastern New Mexico: U. S. Geol. Surv. Open-File Rpt. 85-229, 11 p.
- Walter, J. C., 1953, Paleontology of the Rustler Formation, Culberson County, Texas: *Jour. Paleontology*, v. 27, p. 679-702.

**PLATES**

#### DESCRIPTIONS OF PLATE 1 PHOTOGRAPHS

1. Very-fine grained, muddy sandstone, with lamination disrupted by burrows. S-1 siliciclastic sandstone and mudstone, Lower Member.
2. Very-fine grained laminated muddy sandstone near top of S-1 siliciclastic sandstone and mudstone sequence, Lower Member.
3. Laminated to thin bedded mudstone and very fine grained sandstone, with isolated randomly oriented subhedral to euhedral halite cubes. Near base of the muddy halite (H-1) of the Lower Member.
4. Mudstone-halite from muddy halite (H-1) of the Lower Member.



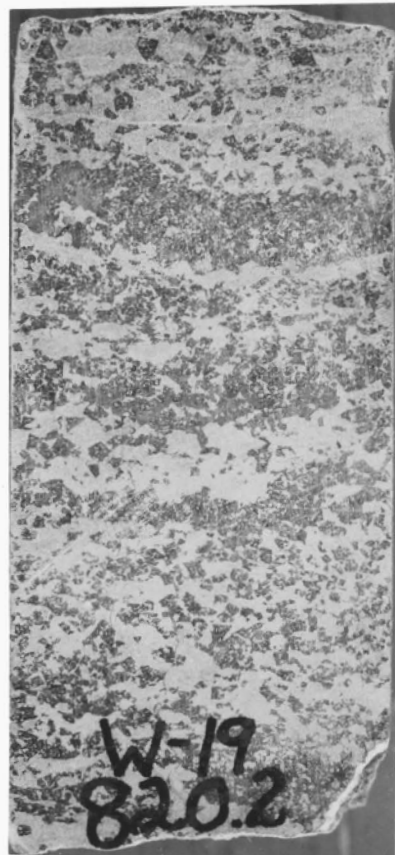
1



2



3



4

DESCRIPTIONS OF PLATE 2 PHOTOGRAPHS

5. Layered halite from the anhydrite-halite sequence (A-H-1) of the Lower Member
6. Mudstone-halite from muddy halite (H-2) of the Lower Member
7. Laminated anhydrite from anhydrite (A-1) of the Lower Member
8. Contact between anhydrite (A-1) and mudstone (I) of the Lower Member

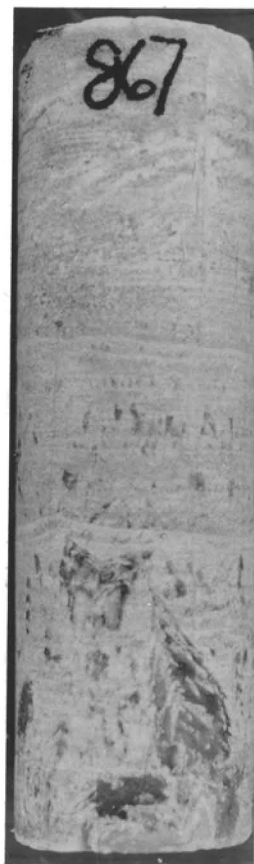




5



6



7



8

DESCRIPTIONS OF PLATE 3 PHOTOGRAPHS

9. Mudstone (I) of the Lower Member.
10. Dolostone from near base of Culebra Dolomite Member.
11. Structureless dolostone from middle part of Culebra Dolomite Member
12. Halite from halite-muddy halite sequence (H-3) of the Tamarisk Member



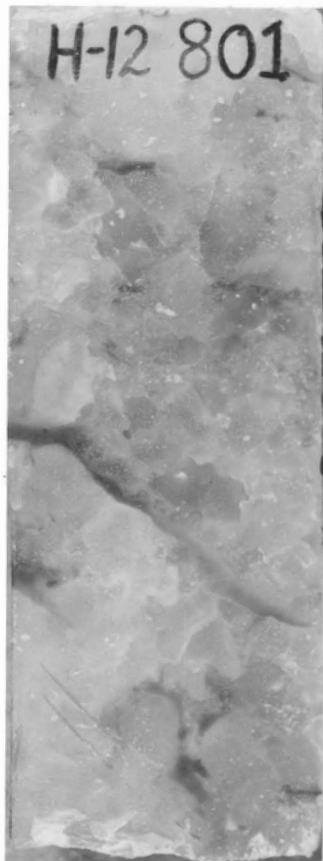
9



10



11



12

DESCRIPTIONS OF PLATE 4 PHOTOGRAPHS

13. Brown mudstone (II) of the Tamarisk Member
14. Chaotic mudstone from Mudstone II of the Tamarisk Member
15. Brown mudstone II of the Tamarisk Member
16. Base of anhydrite (A-3) of the Tamarisk Member



13



14



15



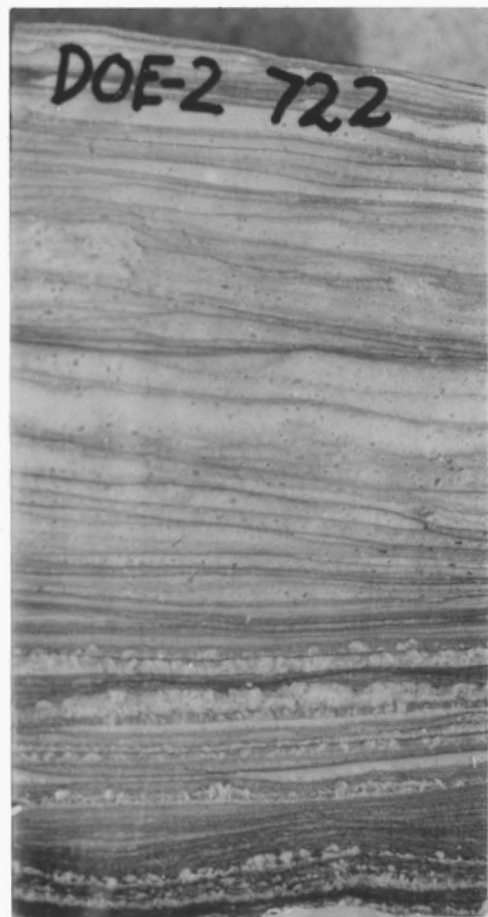
16

DESCRIPTIONS OF PLATE 5 PHOTOGRAPHS

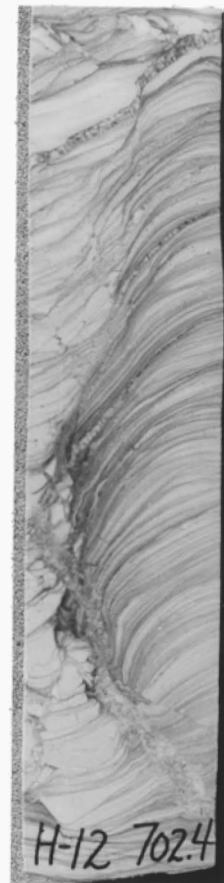
17. Middle portion of anhydrite (A-3) of the Tamarisk Member
18. Laminated dolostone from base of the Magenta Dolomite Member
19. Laminated dolostone from base of Magenta Dolomite Member
20. Laminated to thin bedded dolostone with dark, organic-rich partings from the Magenta Dolostone Member



17



18



19

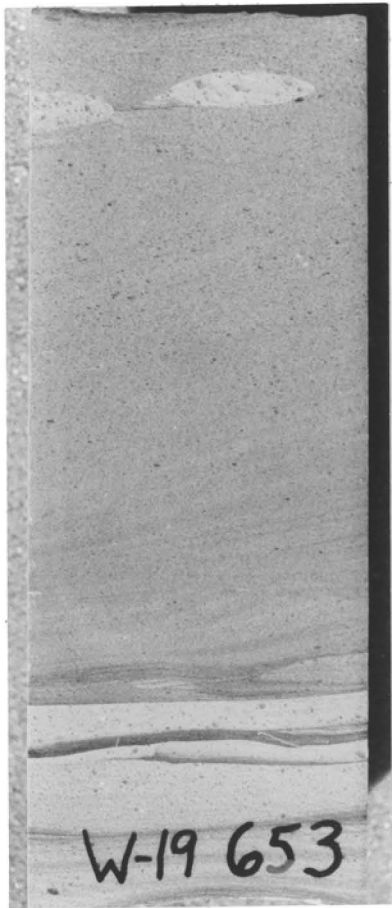


20

DESCRIPTIONS OF PLATE 6 PHOTOGRAPHS

21. Large scale cross stratification in the Magenta Dolomite Member
22. Bottom of anhydrite (A-5), Forty-Niner Member
23. Uppermost portion of A-5 anhydrite, Forty-Niner Member
24. Contact between gypsum of the A-5 anhydrite of the Forty-Niner Member (top of Rustler Formation) and the structureless brown mudstone of the Dewey Lake Formation





21



22



23



24